Available online at www.sciencedirect.com
SCIENCE DIRECT®
Journal of Sound and Vibration 287 (2005) 901–917
JOURNAL OF SOUND AND VIBRATION
www.elsevier.com/locate/jsvi

On the transient dynamics of a multi-degree-of-freedom friction oscillator: a new mechanism for disc brake noise

N.M. Kinkaid, O.M. O'Reilly*, P. Papadopoulos

Department of Mechanical Engineering, University of California, Berkeley, CA 94720-1740, USA

Received 28 April 2004; received in revised form 1 November 2004; accepted 8 December 2004
Available online 24 February 2005

Abstract

In this paper, we examine the dynamics of a simple model for a braking process. The 4 dof model is designed to capture some of the dynamics of a set of brake pads halting a rotor. We find from our model that the motion of the system transverse to the direction of braking experiences a sharp change in excitation when the slip velocity in the braking direction is low. This change results in a complicated vibration which occurs at low slip speeds. In addition, there is often no correlation between the frequencies of the resulting vibration and the natural frequencies of system in the absence of friction. Based on the results from our numerical investigations we are able to propose a new mechanism for disc brake squeal. This mechanism is similar to previously proposed mechanisms in that we view squeal as a friction-induced phenomenon. However, in contrast to the majority of these mechanisms, we are able to encompass the transient, dissipative nature of a braking process.

1. Introduction

Squealing disc brakes have long received a large amount of attention from researchers. This attention is due, of course, to the economics of the related customer complaints, warranty claims, and repairs to disc brake systems, but also to the difficult nature of the problem (see Refs. [1–4]).

*Corresponding author.
E-mail address: oreilly@me.berkeley.edu (O.M. O'Reilly).

0022-460X/$ - see front matter © 2005 Elsevier Ltd. All rights reserved.
doi:10.1016/j.jsv.2004.12.005

Though the literature contains several different theories and a fair amount of controversy, there is little doubt that at its crux, disc brake squeal involves a complex, low amplitude vibration of the braking system resulting from a frictional force. Friction oscillators have occupied scores of researchers who have provided many insightful results (see, for example, Ref. [5]), but it seems that this wealth has not yielded a corresponding amount of traction on the elusive problem of disc brake squeal. Based on studies of these oscillators, many mechanisms for disc brake squeal have been proposed.[1] These include a decreasing μ_k with increasing sliding velocity in Ref. [6], sprag-slip (or kinematic constraint instability) in Refs. [7,8], follower force models in Refs. [9,10], the splitting of doublet modes in Ref. [11], and hammering in Ref. [12]. These mechanisms, while accurate or enlightening in many aspects, do not capture all possible aspects and regimes of disc brake squeal. Of course, some features must be omitted when constructing simple models to explain phenomena as complex as disc brake squeal, but it seems that there have been few attempts to include a more general sliding framework or transient phenomena.

We would like to emphasize that most analyses of disc brake squeal feature a model for the braking system where two contacting bodies have a constant slip velocity field. This is also true in studies of brake creep groan (see Ref. [13]), a brake noise regime in which the magnitude of the slip velocity field approaches zero. The steady state natures of the friction force and slip velocity fields lends these models to an eigenvalue analysis where instability of the steady braking state is equated to brake squeal.[2] The assumption of a steady-state braking event is very limited and excludes the case where the braking event reduces the slip velocity field between the bodies to zero. In this paper, we wish to look at this case. The braking event in which we are interested features stick–slip transitions. These are not amenable to analytics and, consequently, we resort to numerical simulations. These simulations produce some surprising results which are substantially different from those obtained using earlier steady state brake noise models.

As a result of our numerical work with a simple model of a braking system, we propose a new mechanism for disc brake squeal. The mechanism is as follows: During a braking event, we may consider two braking directions, longitudinal and transverse. In an automotive disc brake, the longitudinal direction is the circumferential direction of the brake rotor while the transverse direction is the radial direction of the brake rotor. As the braking event proceeds, the slip velocity (v_{sl}) in the longitudinal direction eventually approaches the same order of magnitude as the slip velocity (v_{st}) in the transverse direction. As v_{sl} passes through zero, the direction of the friction force experiences a sharp change. This change is experienced by modes in the transverse direction as a rapidly varying force which induces vibrations in this direction. It is probable, owing to asymmetries in the rotor geometry and contact conditions and the Poisson effect, that the vibration in the radial direction will lead to out-of-plane vibrations of the rotor. If any of these vibrations are in the audible range, they will contribute to disc brake squeal. The frequencies of vibration do not necessarily correspond to natural frequencies of the stationary, frictionless brake system.

[1]There are numerous such models involving frictional oscillators. In the interests of brevity, we refer the reader to Section 8 of Ref. [1] for a discussion of them.

[2]In the absence of viscous dissipation, the onset of instability is often called *binary flutter* or a *reversible Hopf bifurcation*. An analysis of this type is often referred to as a "complex modal analysis."

An outline of this paper is as follows: In the next section, we present a simple 4 dof model of a brake system. The numerical method we use to examine the stick–slip vibrations of this system is discussed in Section 3. This is followed in Section 4 by our numerical results which lead us to propose our mechanism for disc brake squeal in Section 5. We conclude the paper with a discussion of future research directions and some closing remarks.

2. A four-degree-of-freedom friction oscillator

One of the main purposes of this paper is to analyze the dynamics of a friction oscillator when one of its constituents halts the other. This mimics the behavior of disc brakes where the pads bring the rotor to a stop. Indeed, it can be argued that the model we discuss below is a finite modal truncation of an actual disc brake system.[3] The small number of dof in the model permits us to perform a tractable numerical analysis and infer some interesting conclusions.

Consider the two-mass system shown in Fig. 1. One mass, m_2, is elastically restrained in the y direction by linear springs with constant k_{2y} and is given an initial velocity u_0 in the x direction. This mass is to be braked by frictional interaction with a second mass, m_1, which is elastically restrained by two sets of linear springs k_{1x} and k_{1y}. The two masses are pressed together such that the resultant normal force N exists with the desired (positive) value at all times. The x coordinate of m_1 and both y coordinates are measured from the equilibrium position of the system, while the x coordinate of m_2 measures the net distance traveled by m_2 in the x direction.

An important feature of the model is that the motion of m_2 is not prescribed in any way except that it shall evolve from the imposed initial conditions in accordance with the applicable physical laws, including a constitutive relation for frictional interaction which will be discussed below. We emphasize that although the purpose of the model is to investigate a simple case of decelerative frictional behavior, there is no prescribed deceleration (as, e.g., in Refs. [14–16]).

In the present study, the frictional interaction between the two bodies is governed by the Amontons–Coulomb law. This dictates that if $\mathbf{v}_{\text{rel}}$ is the relative velocity between the two masses and $|\mathbf{v}_{\text{rel}}| > 0$, the friction force $\mathbf{F}_f$ is given by

$$\mathbf{F}_f = -\mu_k N \frac{\mathbf{v}_{\text{rel}}}{|\mathbf{v}_{\text{rel}}|}, \tag{1}$$

where μ_k is the coefficient of kinetic friction, N is the magnitude of the normal force, and $|\cdot|$ denotes the length of a vector. During sticking (i.e., when $|\mathbf{v}_{\text{rel}}| = 0$), the friction force becomes a Lagrange multiplier vector enforcing the constraints

$$\mathbf{v}_{\text{rel}} = \mathbf{0}. \tag{2}$$

If imposing these constraints causes the condition

$$|\mathbf{F}_f| \leqslant \mu_s N, \tag{3}$$

[3]The model described below accommodates two modes in the y direction (corresponding to the radial direction) and one mode in the x (circumferential) direction. By varying the relative natural frequencies of these modes, one may investigate the possible interactions of in-plane modes with widely varying frequencies.

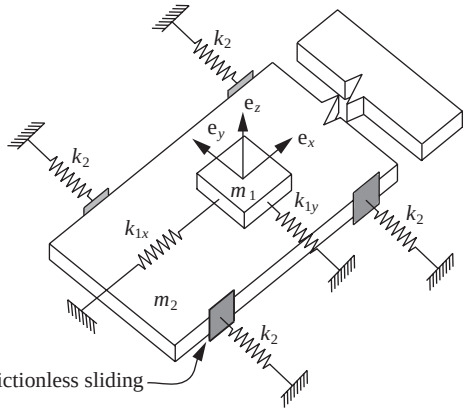

Fig. 1. Schematic of the 4 dof model for a friction oscillator. The body of mass m_2 is given an initial velocity in the $\mathbf{e}_x$ direction and is braked via frictional interaction with the body of mass m_1. The latter is elastically restrained by the springs k_{1x} and k_{1y}. We note that the effective spring constant of all the springs labeled k_2 is k_{2y}.

where μ_s is the coefficient of static friction, to be violated, constraints (2) are relaxed, and the friction force is governed by the slip law (1).

With the friction force prescribed as above, it is straightforward to obtain the equations of motion for the system:

$$\begin{aligned} m_1\ddot{x}_1 &= -k_{1x}x_1 - c_{1x}\dot{x}_1 + F_{fx}, \\ m_1\ddot{y}_1 &= -k_{1y}y_1 - c_{1y}\dot{y}_1 + F_{fy}, \\ m_2\ddot{x}_2 &= F_{fx}, \\ m_2\ddot{y}_2 &= -k_{2y}y_2 - c_{2y}\dot{y}_2 - F_{fy}, \end{aligned} \tag{4}$$

where F_{fx} and F_{fy} represent the x and y components of the friction force, respectively, and the superposed dot signifies differentiation with respect to time. In the interest of increased generality, linear viscous damping (with coefficients c_{1x}, c_{1y}, and c_{2y}) has been also included where appropriate. Using the definitions

$$\begin{aligned} &\tau = t\omega_1, \quad \omega_1 = \sqrt{\frac{k_{1x}}{m_1}}, \quad \omega_2 = \sqrt{\frac{k_{1y}}{m_1}}, \quad \omega_3 = \sqrt{\frac{k_{2y}}{m_2}}, \\ &\delta_{1x} = \frac{c_{1x}}{m_1\omega_1}, \quad \delta_{1y} = \frac{c_{1y}}{m_1\omega_1}, \quad \delta_{2y} = \frac{c_{2y}}{m_2\omega_1}, \\ &\Omega_1 = \frac{\omega_2}{\omega_1}, \quad \Omega_2 = \frac{\omega_3}{\omega_1}, \quad \mathsf{x} = \frac{x\omega_1}{u_0}, \end{aligned} \tag{5}$$

one is immediately led to the non-dimensional equations of motion

$$\begin{aligned} \mathsf{x}_1'' &= -\mathsf{x}_1 - \delta_{1x}\mathsf{x}_1' + \mathsf{F}_{fx}, \\ \mathsf{y}_1'' &= -\Omega_1\mathsf{y}_1 - \delta_{1y}\mathsf{y}_1' + \mathsf{F}_{fy}, \\ \mathsf{x}_2'' &= -\mathsf{F}_{fx}, \\ \mathsf{y}_2'' &= -\Omega_2\mathsf{y}_2 - \delta_{2y}\mathsf{y}_2' - \mathsf{F}_{fy}, \end{aligned} \tag{6}$$

where $(\cdot)'$ signifies differentiation with respect to the non-dimensional time τ. Note that in Eq. (6), the F's denote the dimensionless friction forces, which are found by replacing N with $\mathsf{N} = N/(m_1 u_0 \omega_1)$ in Eqs. (1) and (3).

3. Numerical integration scheme

The prescription of Amontons–Coulomb friction introduces a number of analytical and computational difficulties. Primary among them is that this prescription encompasses two phenomenologically different states, sticking and slipping, for bodies in contact. In each of these states, the friction force must be calculated in a different manner, i.e., directly from Eq. (1) during slipping or as a Lagrange multiplier enforcing the constraint equation (2) during sticking. Additional difficulty is encountered due to inequality (3) that must be used to determine the appropriate state. Thus Amontons–Coulomb friction with stick–slip does not lend itself easily to either closed form analysis or numerical integration.

For the problem at hand, it is convenient to define the state vector

$$\mathbf{Y} = \left[\mathsf{x}_1 \quad \mathsf{x}_1' \quad \mathsf{y}_1 \quad \mathsf{y}_1' \quad \mathsf{x}_2 \quad \mathsf{x}_2' \quad \mathsf{y}_2 \quad \mathsf{y}_2'\right]^{\mathrm{T}}, \tag{7}$$

and recast Eqs. (6) in state-space form as

$$\mathbf{Y}' = \mathbf{G}(\mathbf{Y}, \tau), \tag{8}$$

where dependence on dimensionless time τ is included for generality. The solution of Eqs. (8) must satisfy a pair of algebraic constraints

$$\mathbf{g}(\mathbf{Y}, \tau) = \mathbf{0}, \tag{9}$$

where the vector function $\mathbf{g}$ is given by

$$\mathbf{g}(\mathbf{Y}) = \begin{cases} \mathbf{v}_1 - \mathbf{v}_2 & \text{for sticking states,} \\ \mathbf{F}_f + \mu_k \mathsf{N} \dfrac{\mathbf{v}_1 - \mathbf{v}_2}{|\mathbf{v}_1 - \mathbf{v}_2|} & \text{for slipping states.} \end{cases} \tag{10}$$

In the above,

$$\begin{aligned} \mathbf{v}_i &= \mathsf{x}_i' \mathbf{e}_x + \mathsf{y}_i' \mathbf{e}_y, \quad i = 1, 2, \\ \mathbf{F}_f &= \mathsf{F}_{fx} \mathbf{e}_x + \mathsf{F}_{fy} \mathbf{e}_y. \end{aligned} \tag{11}$$

The system, consisting of Eqs. (8) and (9), may be regarded as a set of differential algebraic equations (DAEs). Such systems are classified by their index m, which is defined as the smallest number of differentiations that are needed in order to transform the system into a purely differential form. If the index of the system of DAEs is less than or equal to 2, the system can usually be solved by the means of methods developed for the solution of systems of ordinary differential equations. It may be seen that the system in question here, Eqs. (8) and (9), has index $m = 1$.

Alternatively, the sticking constraint equation $(10)_1$ may be treated as a purely differential constraint and the slipping constraint equation $(10)_2$ as a prescription for the friction force during sliding. Such a formulation allows one to bypass discussion of DAEs, but it presents some

additional drawbacks. First, the solution space is reduced in dimension during sticking. This entails the removal of the friction force from the equations of motion (6) during sticking states, so an additional calculation is needed in order to evaluate the stick condition equation (3). Second, the set of equations being integrated alternates every time a stick–slip or slip–stick transition takes place. In the DAE formulation, the same equations of motion are integrated at every time step, and the friction forces are automatically recovered as a Lagrange multiplier enforcing constraints (9).

As discussed in Ref. [17], DAEs are common in multi-body dynamics and many other fields in engineering and science. Many solution methods have been developed for DAEs in these settings (see Refs. [18,19]) and for DAEs in rigid body contact dynamics in particular. Here, however, the assumption of persistent contact between the two bodies makes the system closely analogous to elasto-plasticity (see Ref. [20]) (even though elasto-plasticity involves DAEs of index $m = 2$). It is therefore convenient to adapt a solution algorithm from elasto-plasticity based on the familiar implicit two-step backward differentiation formula (BDF2) for ODEs.[4]

Here we briefly summarize the adapted method. The equations of motion (6) for the system may be recast in state-space form (see Eq. (8)) where dependence on non-dimensional time τ is included for generality, and a vector-valued constraint equation (9) that must also be satisfied. Note that the appearance here of two pairs of alternately enforced constraint equations (10), represents a small change from the method described in Ref. [21]. Time discretization using the two-step BDF method then results in the algebraic form

$$\begin{aligned} &\mathbf{Y}_{n+1} = \alpha_{1n}\mathbf{Y}_{n-1} + \alpha_{2n}\mathbf{Y}_n + \beta_n \Delta t_n \mathbf{G}_{n+1}, \\ &\mathbf{g}(\mathbf{Y}_{n+1}) = \mathbf{0}, \end{aligned} \tag{12}$$

where the coefficients α_{1n}, α_{2n}, and β_n are

$$\begin{aligned} \alpha_{1n} &= -\frac{\Delta t_n^2}{\Delta t_{n-1}(\Delta t_{n-1} + 2\Delta t_n)}, \\ \alpha_{2n} &= \frac{(\Delta t_{n-1} + \Delta t_n)^2}{\Delta t_{n-1}(\Delta t_{n-1} + 2\Delta t_n)}, \\ \beta_n &= \frac{\Delta t_{n-1} + \Delta t_n}{\Delta t_{n-1} + 2\Delta t_n}, \end{aligned} \tag{13}$$

and $\Delta t_n = t_{n+1} - t_n$.

Stick is assumed at the outset of every time step (i.e., Eq. $(10)_1$ is assumed to hold at time t_{n+1}). If the previous step described the system as being in stick condition, the states are found at time t_{n+1} using Eq. $(12)_{1,2}$. Otherwise, the two-step method may not be applied, and these values are calculated using the one-step BDF method

$$\mathbf{Y}_{n+1} = \mathbf{Y}_n + \Delta t_n \mathbf{G}_{n+1}, \tag{14}$$

(which is the standard backward Euler method) coupled with Eq. $(12)_2$. If the calculated magnitude of the multipliers needed to enforce the constraint equation $(10)_1$ is greater than the amount of static friction that can be supported, the step is discarded and recalculated using the

[4]Further details on this formula can be found in Ref. [21].

slip constraint equation $(10)_2$. Here, the recalculation is done using BDF2 (*resp.* BDF1) when the previous step described a slip (*resp.* stick) state.

One point from Ref. [21] concerning BDF methods for DAEs that deserves emphasis here is that form (12) has the favorable attribute that the constraints are enforced at the end of every time step. This assures exact satisfaction of the constraints at the same instant at which the momentum equations $(12)_1$ are also satisfied.

4. Results

Before discussing the results of the system investigation, some discussion of initial conditions and parameter selection is warranted. In each of the following examples, the aim is to mimic a braking event. Hence, the large mass (m_2), which is meant to represent the rotor, is given a large initial velocity while the small mass (m_1), which is meant to represent the pads, is initially at rest. Specifically, the large block (m_2) is given an initial x velocity $u_0 = 10$. Additionally, so that effects in the transverse direction might be observed, this block is given a (relatively) much smaller velocity in the y direction: $\mathsf{y}_2'(\tau = 0) = 0.01$.

Parameters are selected in order to investigate the range of possible general behaviors of the system. This means comparing permutations of the ordering $1 < \Omega_1 < \Omega_2$, where the non-dimensional frequencies are typically chosen so as to avoid periodic behavior during sliding phases. The effect of different levels of damping is also investigated. One should note, however, that as $\mu_{s,k}$ and N always appear in concert in this model, it is not possible to separate the effects of varying these parameters. As such, the product of these two parameters is chosen along with the ratio of the two masses after some simple experimentation so as to allow the system to evolve over a conveniently sized time interval.[5] Each simulation is run with different values of the time step to assure that the results are not an artifact of the numerics.

4.1. Case 1: $\Omega_1 = \Omega_2 = 1$

In this example, all of the natural frequencies are equal and damping is absent ($\delta_i = 0, i = 1, 2, 3$). Fig. 2(a) shows the evolution of the longitudinal velocities of the two blocks, which demonstrates the "braking" action of the system. The motion of m_2 excites an oscillation of m_1 at its natural frequency which immediately saturates (see Fig. 2(b)). The frictional interaction of the two components causes m_2 to decelerate in a manner that is almost linear. Once the x velocity of m_2 is less than the saturation velocity of m_1, the system undergoes a series of alternating slip-to-stick and stick-to-slip transitions as the oscillations of m_1 decrease in magnitude within the linear envelope prescribed by the velocity of m_2. Once enough energy is dissipated, the two masses come to a final, persistent sticking state where they oscillate together.

The y velocities show the expected behavior. The small perturbation to the y velocity of m_2 results in both blocks oscillating closely together in the y direction throughout the evolution of the

[5]For the simulations, we choose the dimensionless products of the friction coefficients and the normal force to be 15. Consequently, in all of our simulations $\mu_k = \mu_s$.

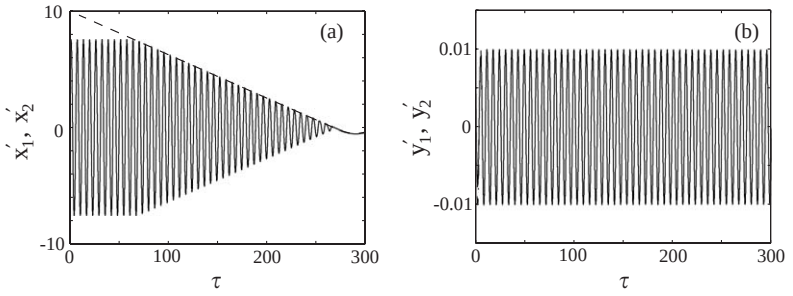

Fig. 2. Case 1: $\Omega_1 = \Omega_2 = 1$. Time histories of the (a) x and (b) y velocities of the system. The solid and dashed lines indicate m_1 and m_2, respectively.

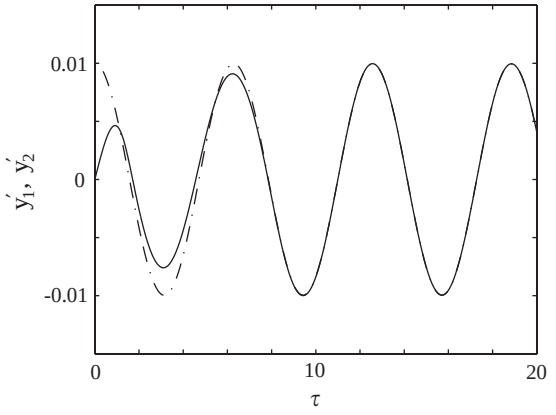

Fig. 3. Case 1: $\Omega_1 = \Omega_2 = 1$. Initial time history of the y velocities. The solid and dashed lines represent m_1 and m_2, respectively.

system. Fig. 3 shows the first part of the velocity response in the y direction. The stick–slip behavior is barely noticeable in the transverse direction (see Figs. 2(b) and 3).

4.2. *Case 2:* $\Omega_2 < 1 < \Omega_1$

In this case, the frequency ratios are $\Omega_1 = 10\sqrt{\pi/2}$ and $\Omega_2 = \frac{1}{100}\sqrt{5/2}$, and damping is again absent. As shown in Fig. 4(a), the braking action of the system in this case is virtually identical to that in Case 1 (see Fig. 2(a)).

However, an interesting behavior manifests itself in the transverse direction. Notice now that with a mismatch in the system's natural frequencies, the small perturbation in the y direction results in a somewhat peculiar looking oscillation of m_1 as shown in Fig. 4(c). The response is characterized by a periodic series of strong spikes within an envelope interspersed with much

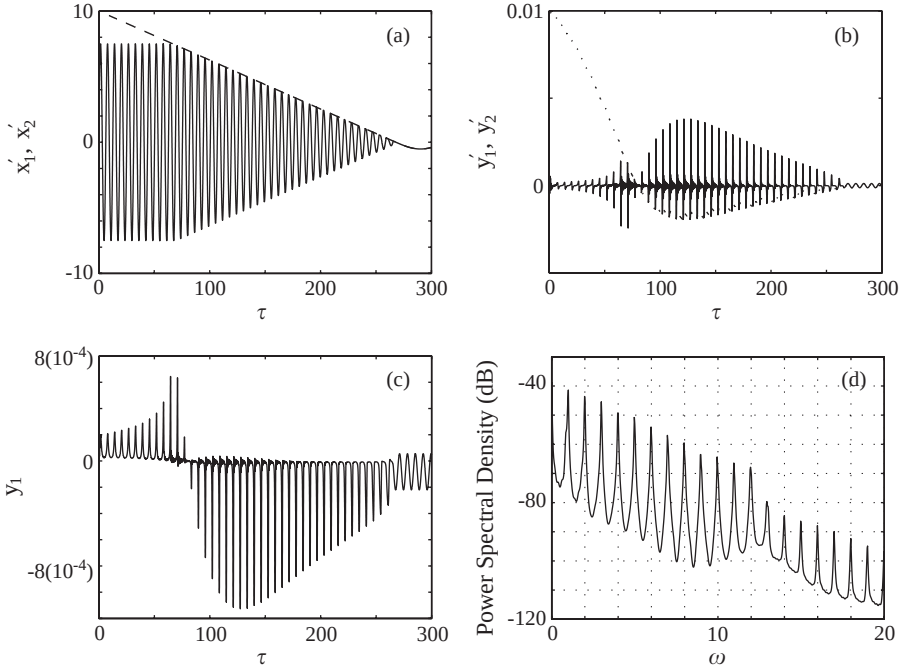

Fig. 4. Case 2: $\Omega_1 = 10\sqrt{\pi/2} \approx 12.53$ and $\Omega_2 = \frac{1}{100}\sqrt{5/2} \approx 0.016$. Time histories of the (a) x and (b) y velocities of both masses, and (c) y position of m_1. The approximate power spectral density of the y response of m_1 (as appears in (c)) is shown in (d). Solid lines indicate m_1 and dashed lines m_2.

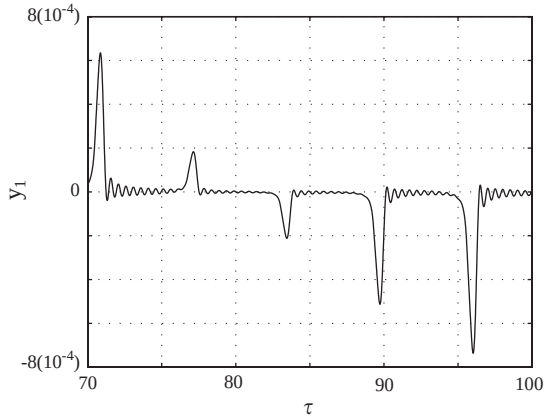

Fig. 5. Case 2: $\Omega_1 = 10\sqrt{\pi/2} \approx 12.53$ and $\Omega_2 = \frac{1}{100}\sqrt{5/2} \approx 0.016$. Time series of the y position of block m_1.

smaller decaying oscillations at a higher frequency. Fig. 5 shows a few of these oscillations in greater detail.

Perhaps more insight into the behavior can be gained from attention to the frequency response. Fig. 4(d) shows the power spectral density of the y response of m_1 as obtained by the maximum entropy method (see Refs. [22,23]). The frequency response of m_1 in the transverse direction is

dominated by a decaying train of regularly spaced spikes. According to Ref. [24], the frequency response of periodically spaced impulse functions, say

$$f(t) = \delta(nT), \quad n = 1, 2, 3, \ldots, \tag{15}$$

is a series of impulse functions separated by $1/T$:

$$\mathscr{F}(\omega) = \delta\left(n\frac{1}{T}\right), \quad n = 1, 2, 3, \ldots, \tag{16}$$

where $\delta(\cdot)$ is the Dirac delta function. Note that the spacing of the spikes in Fig. 4(d) is equal to 1, which is the natural frequency of m_1 in the x direction. It is also interesting to note that the decay of the spikes becomes stronger past the natural frequency of m_1 in the y direction (which is approximately equal to 12.5), and that there is *no* peak at that frequency.

4.3. *Case 3:* $1 < \Omega_1 < \Omega_2$

Now observing the case where $\Omega_1 = 2\sqrt{5}$ and $\Omega_2 = 5\sqrt{2}$, again with no viscous damping, we find that once again the velocities in the x direction (see Fig. 6(a)) respond indistinguishably from what is shown in Fig. 2(a). This means that the braking action is unaffected. Once again, though, the y response of m_1 (see Fig. 6(b)) shows a complicated, multi-scale vibratory response. The mismatch of natural frequencies here results in another impulse-train-like transverse response for m_1.

Fig. 7 shows this frequency response. Again, peaks separated by $\Delta\omega = 1$ are observed. These peaks increase in magnitude in the range $\Omega_1 < \omega < \Omega_2$ and decrease when the frequency becomes higher than Ω_2. Once again the response of m_1 in the y direction shows no peak at the natural frequency for the uncoupled system in that direction. It should be noted that the peaks do not actually occur at multiples of 1, but rather are shifted to the right. In fact, the shifting is equal to $\Omega_2 \approx 7.07$, so the apparent shift is only approximately 0.07.

Here, then, it is illuminating to apply the Frequency Shifting Theorem, which states [24] that if the Fourier transform of $f(t)$ is $\mathscr{F}(\omega)$, then the Fourier transform of $e^{j\omega_0 t}f(t)$ is $\mathscr{F}(\omega - \omega_0)$, and vice versa. Thus, one can interpret that in this case, the transverse impulse train to which m_1 is

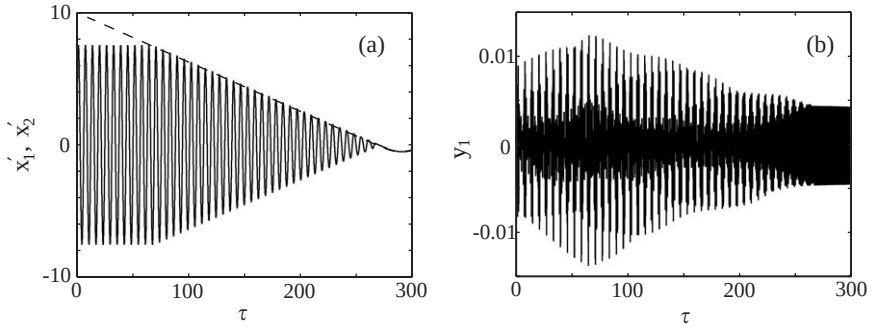

Fig. 6. Case 3: $\Omega_1 = 2\sqrt{5} \approx 4.47$ and $\Omega_2 = 5\sqrt{2} \approx 7.07$. Time history of the (a) x velocities (solid line for m_1 and dashed line for m_2) and (b) y position of m_1.

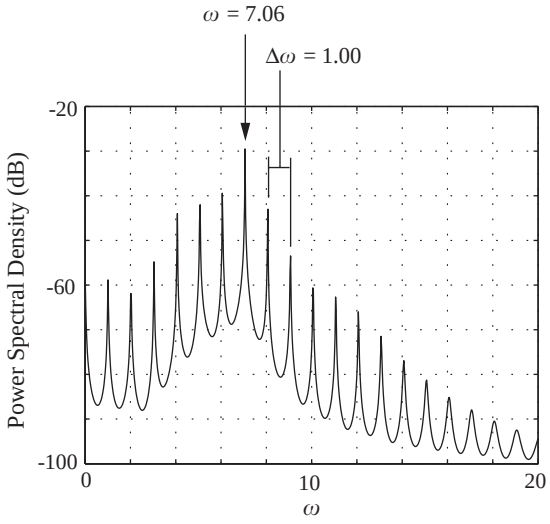

Fig. 7. Case 3: $\Omega_1 = 2\sqrt{5} \approx 4.47$ and $\Omega_2 = 5\sqrt{2} \approx 7.07$. Approximate power spectral density of the y response of m_1. The indicated values of ω are taken from the peak values of the approximate power spectral density.

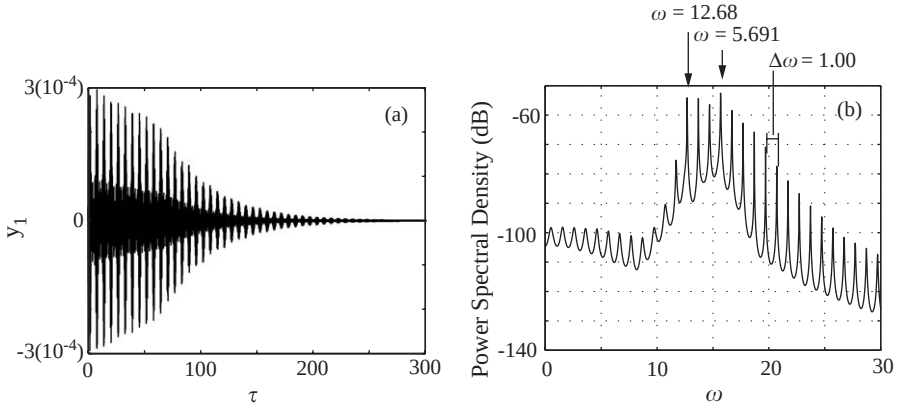

Fig. 8. Another example of Case 3: $\Omega_1 = 10\sqrt{\pi/2} \approx 12.53$ and $\Omega_2 = 10\sqrt{5/2} \approx 15.81$. Time series of y_1 (a) and the corresponding approximate power spectral density (b). The values of ω indicated in (b) are taken from the peak values of the approximate power spectral density.

subjected is modulated by a trigonometric function with frequency $\omega_0 = 7.07 \approx \Omega_2$. Indeed, it may be inferred that this effect appears in Case 2 above as well, but there Ω_2 is so small (≈ 0.016) that the effect is negligible.

In order to emphasize this point, we present here some results from another case with $1 < \Omega_1 < \Omega_2$, specifically $\Omega_1 = 10\sqrt{\pi/2}$ and $\Omega_2 = 10\sqrt{5/2}$. As seen in Fig. 8(b), the spectrum is shifted by roughly $\Omega_2 \approx 15.81$. The y response of m_1 for this case is shown in Fig. 8(a).

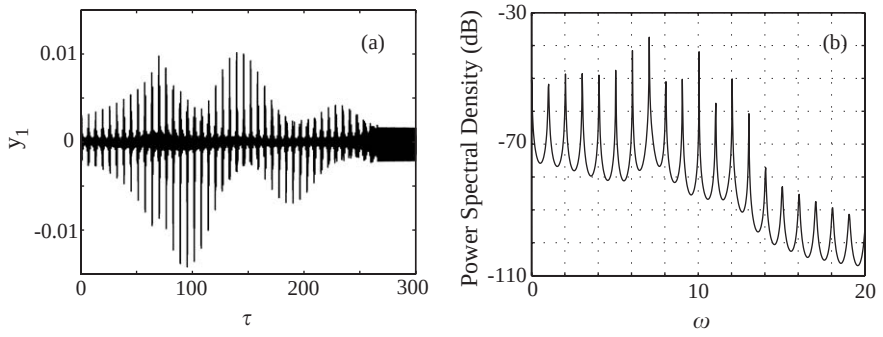

Fig. 9. Case 4: $\Omega_1 = 10\sqrt{\pi/2}$ and $\Omega_2 = 5\sqrt{2}$. (a) Time history of the y position of block m_1, and (b) power spectral density estimate of y response.

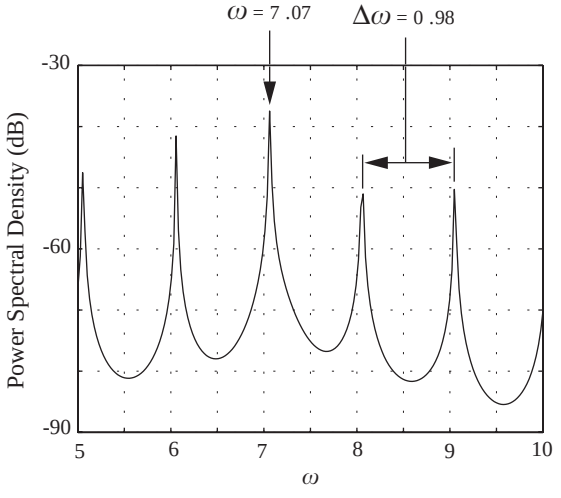

Fig. 10. Case 4: $\Omega_1 = 10\sqrt{\pi/2} \approx 12.53$ and $\Omega_2 = 5\sqrt{2} \approx 7.07$. Power spectral density of y position of block m_1.

4.4. *Case 4:* $1 < \Omega_2 < \Omega_1$

Here again we examine the behavior of the system with no viscous damping. In this case, the frequency ratios Ω_1 and Ω_2 are $10\sqrt{\pi/2}$ and $5\sqrt{2}$, respectively. As expected, the braking action remains entirely similar to that shown in Fig. 6(a). Fig. 9(a) shows the transverse response for m_1. Again, there is insight to be gained by transforming this data to the frequency domain (see Fig. 9(b)) where the familiar impulse train structure is seen. The peaks tend to increase until $\omega \approx \Omega_2$, then decrease, the rate of attenuation increasing after $\omega \approx \Omega_1$. The spectrum is once again shifted by Ω_2, which is demonstrated more clearly in Fig. 10, where a portion of the power spectral density is shown in greater detail.

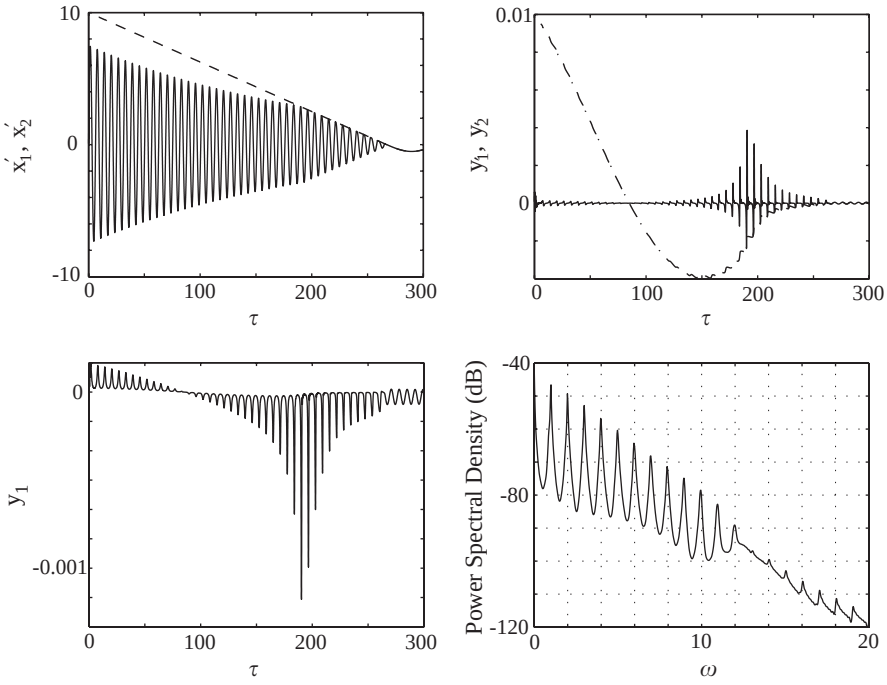

Fig. 11. Case 5: $\Omega_1 = 10\sqrt{\pi/2}$ and $\Omega_2 = \frac{1}{100}\sqrt{5/2}$, and $\delta_i = 0.01, (i = 1, 2, 3)$. (a) x velocities, (b) y velocities, (c) y position of m_1, and (d) the approximate power spectral density of the time history of y_1. For comparison, Fig. 4 shows this data for the undamped version.

4.5. Case 5: Effects of Viscous Damping

In order to investigate the effects of viscous damping in the system, the natural frequencies are set to those of Case 2 above (namely $\Omega_1 = 10\sqrt{\pi/2}$, $\Omega_2 = \frac{1}{100}\sqrt{5/2}$) and a moderate amount of viscous damping is added ($\delta_i = 0.01, i = 1, 2, 3$). As seen in Fig. 11, this amount of viscous damping attenuates but does not eliminate the impulse-train-like response. The onset of this type of response is delayed by the damping due to the attenuation of oscillations of m_1 in the longitudinal direction.

5. A mechanism for brake squeal

Clearly, the behavior of the model presented above shows that under suitable conditions, a sliding system may be subjected to periodic impulses in the direction perpendicular to the predominant sliding velocity. However, further examination is necessary to explain how these impulses manifest.

When the system is set in motion as described at the outset of Section 4, the sliding velocity is dominated by the action of the system along the longitudinal direction. Initially the small

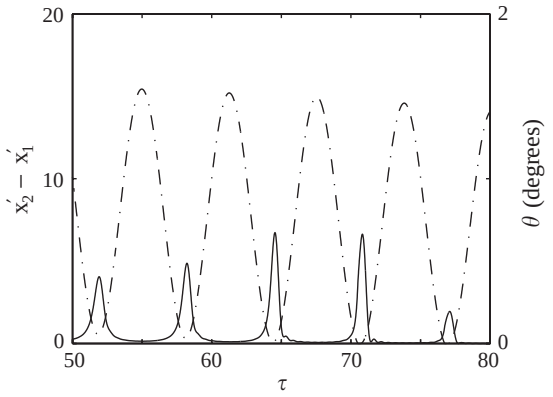

Fig. 12. Relative x velocity (dashed line) and friction force angle θ (solid line) as measured counter-clockwise from $\mathbf{e}_x$ for Case 2: $\Omega_1 = 10\sqrt{\pi/2}$ and $\Omega_2 = \frac{1}{100}\sqrt{5/2}$.

oscillations of the system in the lateral direction have a negligible effect on the overall sliding direction (which corresponds directly to the direction of the friction force when $|\mathbf{v}_{\text{rel}}| > 0$ as seen in Eq. (1)). From Fig. 4(a), one can infer how the x component of $\mathbf{v}_{\text{rel}}$ evolves. As the frictional interaction dissipates energy from the system, oscillations of m_1 in the x direction periodically cause the x component of $\mathbf{v}_{\text{rel}}$ to become small (or even zero as the system progresses into stick–slip motion). When this occurs, the y component of the slip velocity may no longer be negligible, and the direction of the friction force may change suddenly.

Fig. 12 shows how the direction of the friction force (labeled θ and measured in degrees from the x-axis) corresponds to the x component of the sliding velocity during a short interval. This figure seems to support the above hypothesis: each peak in θ coincides with a valley in the x component of $\mathbf{v}_{\text{rel}}$. While the change in friction force direction seen here is less than 1°, this imparts enough momentum to m_1 in the y direction to cause the behavior discussed in Section 4. Some important features to be noted in Fig. 12 are that this effect occurs both before and after the onset of stick–slip motion, that the height of the θ peaks tends to grow with the deepening of the valleys in the x component of $\mathbf{v}_{\text{rel}}$ (though the height is also dependent upon the y component), and that the peaks in θ tend to slightly lag the valleys in $\mathbf{v}_{\text{rel}} \cdot \mathbf{e}_x$.

One interpretation of the lateral impulse trains witnessed in the previous section allows for the description of a mechanism for disc brake noise that is in many ways consistent with the known qualitative aspects of that phenomenon. Foremost, the impulse trains can only occur when the forward speed of m_2 is low, corresponding to a low forward speed of a vehicle. The low-speed nature of brake squeal is one of its most important aspects, yet the authors know of no proposed mechanism which addresses it.

Secondly, it has been noted (see Section 2.3 of Ref. [1], for example) that the sound power of disc brake squeal represents a minuscule fraction of the mechanical power being dissipated in a braking action. Results in Section 4 show clearly that the action of this mechanism, which is entirely in the lateral direction, is orders of magnitude less than the action of the main braking

effect, which takes place in the longitudinal direction. The transfer of power from braking into other effects here seems to be inherently limited, which is a feature missing from linear stability based models.

An interesting note is that the system under examination here supports only one motion as time tends toward infinity. With the damping parameters set to any values greater than zero, the system eventually comes to rest. Otherwise, a bounded harmonic oscillation results. In either case, the system is stable, yet squeal may still result during the transient stages if the ratios of the natural frequencies favor it.

One aspect that our mechanism shares with sprag-slip and the follower force models is the excitation of brake squeal through the variation of the friction force as the coefficient of kinetic friction remains constant. In these two models, this effect is achieved through the variation of the magnitude of the friction force by varying the normal force on which it linearly depends. In our newly proposed mechanism, it is changes in the direction rather than the magnitude of the friction force which are supposed to excite squeal. It is not unreasonable to suppose that some combination of these effects may provide a mechanism which models brake squeal with yet more fidelity.

6. Closing remarks

Although the motivation for our mechanism is based on studies of a rather simple model for a brake system, we are pursuing a more realistic finite-element model of an automotive disc brake. The transient phenomena and multiple length scales involved in this model have made this a difficult model to simulate.

The mechanism we propose has several features in common with recent works by Pilipchuk and Tan (see Refs. [15,16]). These authors also present a transient analysis of a braking event and correlate the resulting creep-slip dynamics to a proposed mechanism for brake squeal.[6] The major differences between the two mechanisms is that ours depends crucially on two-dimensional contact and does not require a μ_k which depends on the sliding velocity dependent. Several authors (see, e.g., Refs. [14–16,25]) have noted the complex spectral response of friction oscillators. However, to our knowledge, the structure we found for the oscillator in this paper is unique.

Our proposed mechanism is similar to the Rhee et al.'s hammering theory of brake squeal (see Ref. [12]). However, their theory is based on a spragging phenomena whereas this is absent in our mechanism. We also emphasize that the vibration frequencies observed in our simple model do not necessarily correspond to the natural frequencies of the system. This suggests that it is not possible to easily predict the squeal frequencies excited by our mechanism. In particular, studying the natural frequencies of rotors and pads may not lead directly to estimates of the squeal frequencies excited by our mechanism.

[6]In Refs. [15,16], a regularization of (one-dimensional) Amontons–Coulomb friction is used. This leads to a parameter regieme where μ_k decreases with increasing sliding velocity.

Acknowledgements

This work was supported by the National Science Foundation under Grant No. CMS0084808. Any opinions, findings, and conclusions or recommendations expressed in this material are those of the authors and do not necessarily reflect the views of the National Science Foundation.

The authors are also grateful to Professor Philip S. Marcus for pointing out the maximum entropy method as a means of spectral analysis, two (anonymous) reviewers for their constructive criticisms, and Professor Brian F. Feeny for his help with the literature.

References

[1] N.M. Kinkaid, O.M. O'Reilly, P. Papadopoulos, Automotive disc brake squeal, *Journal of Sound and Vibration* 267 (1) (2003) 105–166.
[2] S. Yang, R.F. Gibson, Brake vibration and noise: reviews, comments, and proposals, *International Journal of Materials and Product Technology* 12 (1997) 496–513.
[3] R.A. Ibrahim, Friction-induced noise and related problems in automotive brakes, in: S.G. Pandalai (Ed.), *Recent Research Developments in Sound and Vibration*, Vol. 1, Transworld Research Network, Kerala, India, 2002.
[4] A. Papinniemi, J.C.S. Lai, J. Zhao, L. Loader, Brake squeal: a literature review, *Applied Acoustics* 63 (4) (2002) 391–400.
[5] A. Akay, Acoustics of friction, *Journal of the Acoustical Society of America* 111 (4) (2002) 1525–1548.
[6] H.R. Mills, Brake squeak, Technical Report 9000 B, Institution of Automobile Engineers, 1938.
[7] R.T. Spurr, A theory of brake squeal, *Proceedings of the Automobile Division of the Institution of Mechanical Engineers* 1961–1962 (1) (1961) 33–52.
[8] S.W.E. Earles, G.B. Soar, Squeal noise in disc brakes, in: *Vibration and Noise in Motor Vehicles*, Institution of Mechanical Engineers, London, England, 1971, pp. 61–69 Paper number C 101/71.
[9] M.R. North, Disc brake squeal, in: *Braking of Road Vehicles*, Automobile Division of the Institution of Mechanical Engineers, Mechanical Engineering Publications Limited, London, England, 1976, pp. 169–176.
[10] H. Ouyang, J.E. Mottershead, D.J. Brookfield, S. James, M.P. Cartmell, T. Kaster, T. Treyde, B. Hirst, R. Allen, Dynamic instabilities in a simple model of a car disc brake, Technical Report 1999–01–3409, SAE, Warrendale, PA, 1999.
[11] J.E. Mottershead, S.N. Chan, Brake squeal—an analysis of symmetry and flutter instability, in: R.A. Ibrahim, A. Soom (Eds.), *Friction-Induced Vibration, Chatter, Squeal and Chaos*, Vol. DE-49, ASME, New York, 1992, pp. 87–97.
[12] S.K. Rhee, P.H.S. Tsang, Y.S. Wang, Friction–induced noise and vibration of disc brakes, *Wear* 133 (1989) 39–45.
[13] J. Brecht, W. Hoffrichter, A. Dohle, Mechanisms of brake creep groan, Technical Report 973026, SAE, Warrendale, PA, 1997.
[14] P. Vielsack, Stick–slip instability of decelerative sliding, *International Journal of Non-Linear Mechanics* 36 (2001) 237–247.
[15] V.N. Pilipchuk, C.A. Tan, Investigation of a friction-induced source of excitation in disc brake systems, in: *Proceedings of IMECE2002: ASME International Mechanical Engineering Congress & Exposition*, November 17–22, 2002, New Orleans, Lousiana, IMECE2002-32400, ASME International, 2002.
[16] V.N. Pilipchuk, C.A. Tan, Creep-slip capture as a possible source of squeal during decerated sliding, *Nonlinear Dynamics* 35 (2004) 259–285.
[17] E. Eich-Soellner, C. Führer, *Numerical Methods in Multibody Dynamics*, Eigendruck, Lund and Stuttgart, 2002.
[18] L.R. Petzold, Recent developments in the numerical solution of differential/algebraic systems, *Computational Methods in Applied Mechanics and Engineering* 75 (1989) 77–89.
[19] K.E. Brenan, S.L. Campbell, L.R. Petzold, *Numerical Solution of Initial-Value Problems in Differential-Algebraic Equations*, SIAM, Philadelphia, 1996.

[20] A. Curnier, A theory of friction, *International Journal of Solids and Structures* 20 (1984) 637–647.
[21] P. Papadopoulos, R.L. Taylor, On the application of multi-step integration methods to infinitesimal elastoplasticity, *International Journal for Numerical Methods in Engineering* 37 (1994) 3169–3184.
[22] R.A. Haddad, T.W. Parsons, *Digital Signal Processing: Theory, Applications, and Hardware*, Computer Science Press, New York, 1991.
[23] W.H. Press, S.A. Teukolsky, W.T. Vetterling, B.P. Flannery, *Numerical Recipes in C: The Art of Scientific Computing*, second ed., Cambridge University Press, Cambridge, 1994.
[24] A.V. Oppenheim, R.W. Schafer, *Discrete-Time Signal Processing*, second ed., Prentice-Hall, Upper Saddle River, NJ, 1999.
[25] J.W. Liang, B.F. Feeny, Wavelet analysis of stick–slip in an oscillator with dry friction, in: *1995 Design Engineering Technical Conferences*, Vol. 3-A of DETC95/Vol. 84-1, ASME, New York, 1995, pp. 1061–1069.